

Neutron scattering studies on ionic diffusion behaviors of superionic α -Cu_{2- δ} Se

Lisi Li,¹ Huili Liu,² Maxim Avdeev,³ Dehong Yu,³ Sergey Danilkin,³ and Meng Wang^{1,*}

¹Center for Neutron Science and Technology, Guangdong Provincial Key Laboratory of Magnetoelectric Physics and Devices, School of Physics, Sun Yat-Sen University, Guangzhou, 510275, China

²School of Physical Science and Technology, ShanghaiTech University, Shanghai, 201210, China

³Australian Nuclear Science and Technology Organisation, New Illawarra Road, Lucas Heights NSW 2234, Australia.

We present studies on crystal structure and ionic diffusion behaviors of superionic Cu_{2- δ} Se ($\delta=0, 0.04, \text{ and } 0.2$) by utilizing neutron powder diffraction and quasi-elastic neutron scattering. In the superionic phase, the structural model with Cu ions occupying the Wyckoff sites of $8c$ and $32f$ provides the best description of the structure. As the content of Cu increasing in Cu_{2- δ} Se, the Cu occupancy increases on the $32f$ site, but decreases on the $8c$ site. Fitting to the quasi-elastic neutron scattering spectra reveals two diffusion modes, the localized diffusion between the $8c$ and $32f$ sites and the long-range diffusion between the adjacent $8c$ sites using the $32f$ site as a bypass, respectively. Between 430 and 650 K, we measured that the compound with more Cu content exhibits a larger long-range diffusion coefficient. Temperature in this range does not affect the long-range diffusion process obviously. Our results suggest the two diffusion modes cooperative and thus provide a microscopic understanding of the ionic diffusion of the Cu ions in superionic Cu_{2- δ} Se.

PACS numbers:

Thermoelectric (TE) materials that could convert heat to electricity provide a way for waste heat recycle¹. The dimensionless figure of merit $zT = S^2\sigma T/\kappa$ is a measure of the efficiency of TE materials in application, where S , σ , T , and κ are the Seebeck coefficient, electrical conductivity, temperature, and thermal conductivity, respectively^{2,3}. The zT values for high performance TE materials can be higher than 2¹, for instance, SnSe⁴, PbTe^{5,6}, CoSb₃⁷, and Cu₂Se^{8,9}. To obtain an ultra-low thermal conductivity is an important way to achieve a high zT value for TE materials^{4,8}.

Cu_{2- δ} Se is a high performance TE material, hosting a high temperature superionic α -phase and a low temperature localized β -phase with a phase transition at 414 K for $\delta = 0$ ¹⁰⁻¹³. The transition temperature decreases as the increasing of the Cu deficiency δ . In the stabilized β -phase, Cu_{2- δ} Se crystallizes into a monoclinic structure, where the Cu ions form a localized order structure. In the superionic α -phase, Cu_{2- δ} Se forms a cubic structure with the space group $Fm\bar{3}m$ (No. 225). The zT value can reach up to 2.5 for Cu₂Se due to the ultra-low thermal conductivity^{8,9}. The ultra-low thermal conductivity may relate to the ionic diffusion behaviors of the Cu ions in Cu_{2- δ} Se⁸. It is therefore important to investigate the diffusion behaviors of Cu_{2- δ} Se for elucidation the relation between the Cu diffusion and the ultra-low thermal conductivity. However, there are significant discrepancies among the experimental determined diffusion coefficients (D), which are an important parameter for evaluating the diffuse behaviors. The diffusion coefficient was determined to be on the scale of 10^{-7} cm²/s using quasi-elastic neutron scattering (QENS)¹⁴, smaller by two orders of magnitude than the values determined by chemical and other QENS experiments¹⁵⁻²⁰. The discrepancies in diffusion coefficient may originate from different diffusion models in analyzing the QENS data. In addition, the

specific diffusion paths of the Cu ions are under debates. Therefore, careful analyses of the diffusion coefficient is crucial for understanding the diffusion process and the mechanism of the ultra-low thermal conductivity in superionic Cu_{2- δ} Se.

Here we present detailed investigations on the crystal structure and diffusion behaviors of superionic Cu_{2- δ} Se ($\delta = 0, 0.04, 0.2$) using neutron powder diffraction (NPD) and QENS. The refined averaged structure can be described well by a structural model with two Wyckoff sites of $8c$ ($1/4, 1/4, 1/4$) and $32f$ (x, x, x) ($0.331 \leq x \leq 0.337$) for Cu ions [Fig. 1]. The QENS signals arising from the diffusion of Cu ions are observed in the superionic phase. Through our QENS data, a long-range jump diffusion mode and a localized confined mode are obtained. For the long-range diffusion mode, the residence time τ and averaged jump length l are extracted from the Chudley-Elliott (C-E) model²¹. The residence time τ is on the time scale of 10^{-12} s and becomes shorter for the higher Cu content. The averaged jump length l is in the range of 2.7–3.4 Å that could capture the main jump paths of Cu ions diffusing between the adjacent $8c$ sites. In addition, the diffusion coefficient D is on the order of magnitude 10^{-5} cm²/s. The localized confined mode corresponds to the diffusion between the nearest $8c$ and $32f$ sites which is cooperative with the long-range diffusion mode. Our results reveal the influence of Cu content on the Cu ions diffusion process and demonstrate that the liquid-like mobilities of Cu ions are prominent in Cu_{2- δ} Se.

Powder samples of Cu_{2- δ} Se ($\delta = 0, 0.04, 0.2$) were synthesized using the standard solid-state reaction method as in previous reports^{17,18,22}. Starting materials of Cu and Se powder were mixed in the stoichiometric quantities and sealed in quartz tubes under vacuum, which were then placed into a box furnace and heated at 1000 °C for 7 days. The NPD data were collected on the

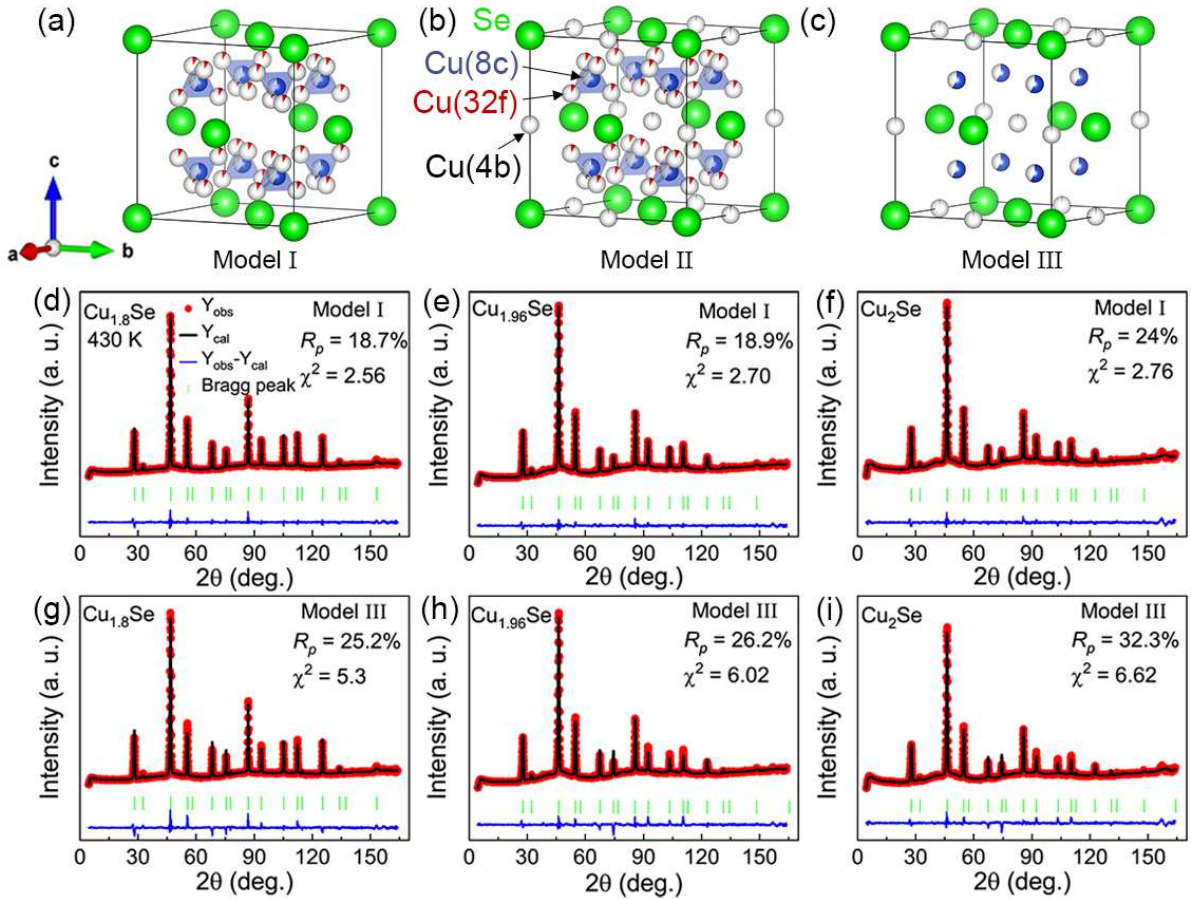


FIG. 1: (a) Structural models for describing α - $\text{Cu}_{2-\delta}\text{Se}$. Model I: Cu ions occupy the 8c and 32f sites. (b) Model II: Cu ions occupy the 8c, 32f, and 4b sites. (c) Model III: Cu ions occupy the 8c and 4b sites. (d) Observed and calculated neutron diffraction patterns at 430 K for $\text{Cu}_{1.8}\text{Se}$, (e) $\text{Cu}_{1.96}\text{Se}$, and (f) Cu_2Se using Model I. (g-i) Comparisons between the identical observed neutron diffraction patterns and calculated patterns using the Model III. The refinement agreement factors R_p and χ^2 have been listed on the figures (d-i).

high resolution powder diffractometer Echidna installed at the OPAL reactor of the Australian Nuclear Science and Technology Organisation (ANSTO)²³. The incident neutron wavelength was $\lambda=1.622$ Å. The Rietveld method was employed to analyze the NPD data using the *FullProf* Suite software²⁴.

The QENS experiments were conducted on the time-of-flight spectrometer Pelican at ANSTO with an incident neutron wavelength of $\lambda=4.69$ Å (3.72 meV) and different chopper configurations²⁵. The powder samples were loaded into sealed aluminum sample cans. The measured temperatures were 430, 550, and 650 K for $\text{Cu}_{1.8}\text{Se}$ and $\text{Cu}_{1.96}\text{Se}$, and 430 and 650 K for Cu_2Se . An empty aluminum sample can was measured at the same temperatures for background subtraction. The spectra of a vanadium cylinder with 1 mm thick were measured to serve as resolution functions in analyzing the QENS spectra using the program *LAMP*²⁶. The energy resolutions determined by the full width at half maximum (FWHM) of the elastic peak of vanadium at $Q = 1.05 \pm 0.15$ Å is 207.8(9) μeV for the earlier measurements on Cu_2Se and

138.9(5) μeV for the later measurements on $\text{Cu}_{1.8}\text{Se}$ and $\text{Cu}_{1.96}\text{Se}$.

The Cu ions of $\text{Cu}_{2-\delta}\text{Se}$ can diffuse through the Se cubic lattice in the superionic α -phase^{27–29}. Diffraction data based on structure refinement can only capture the time- and space-averaged positions of Cu ions in this phase. Three structural models have been proposed for describing the distribution of the Cu ions in the superionic phase, as shown in Figs. 1(a)-1(c). Model I is that the Cu ions occupy the tetrahedral sites 8c ($1/4, 1/4, 1/4$) and trigonal sites 32f (x, x, x) ($x = 0.33 - 0.39$)^{17,18,30,31}. Model II states that most of the Cu ions occupy the tetrahedral sites 8c and the trigonal sites 32f, and a small amount of Cu ions sit in the octahedral sites 4b ($1/2, 1/2, 1/2$)^{32–35}. Model III allows the Cu ions to occupy the sites of 8c and 4b, while the 32f sites are not occupied¹⁹.

To investigate the occupancy of the Cu ions, we conducted NPD measurements. Figures 1(d)-1(f) show the NPD and refined patterns for $\text{Cu}_{2-\delta}\text{Se}$ ($\delta = 0, 0.04, 0.2$) at 430 K in the superionic α -phase using the Model I. The

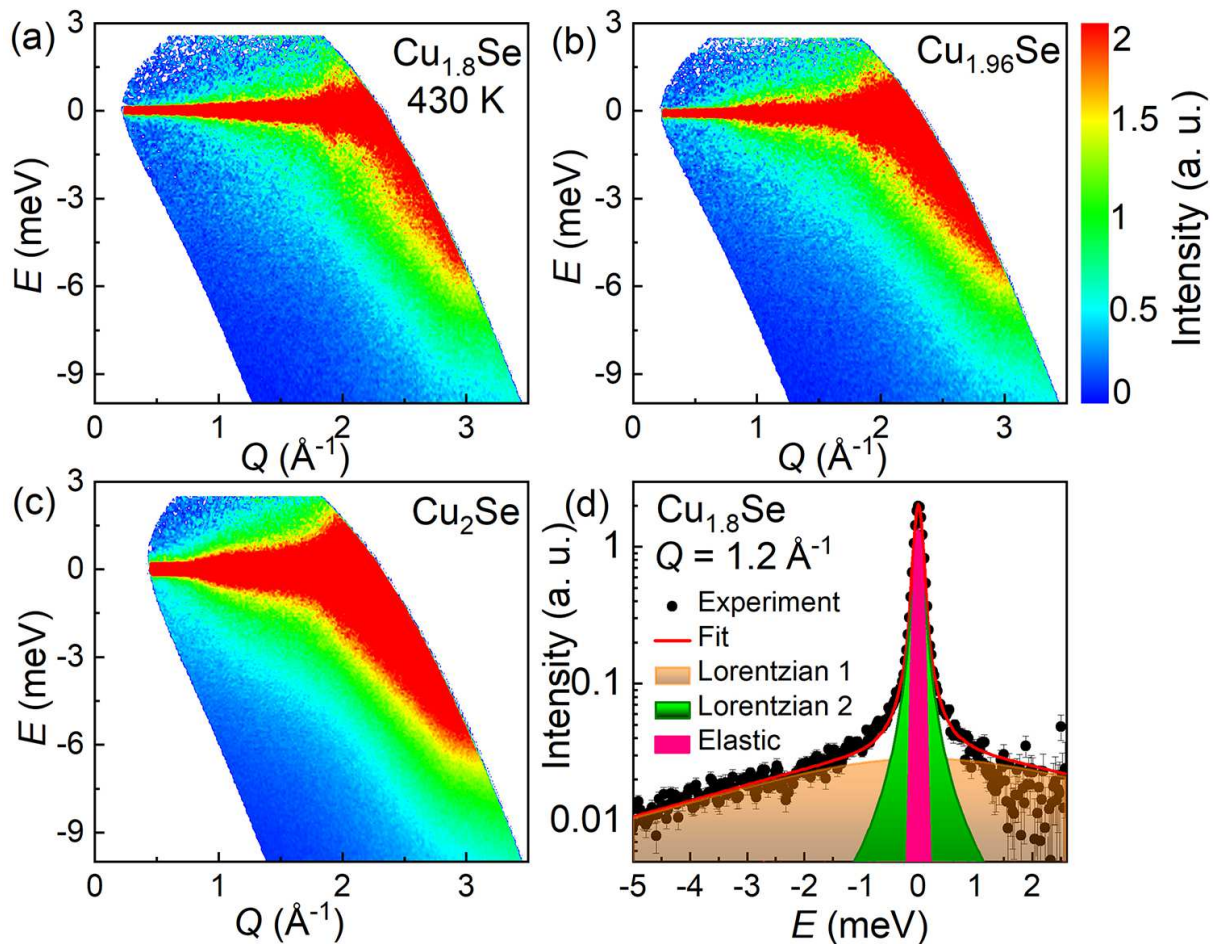


FIG. 2: The QENS spectra measured at 430 K for (a) $\text{Cu}_{1.8}\text{Se}$, (b) $\text{Cu}_{1.96}\text{Se}$, and (c) Cu_2Se . The color represents intensities. (d) Black symbols are a constant Q cut at $Q = 1.2 \text{ \AA}^{-1}$ integrated within $Q \pm 0.075 \text{ \AA}^{-1}$ at 430 K for $\text{Cu}_{1.8}\text{Se}$. The red solid line represents a fitting result of the QENS peak. The orange, green, and pink areas represent the Lorentzian 1, Lorentzian 2, and elastic components of the fitting.

TABLE I: The nominal and refined compositions, the occupancies (Occ.) of Cu ions on the $8c$ and $32f$ sites, and the lattice constant a using the Model I at 430 K for $\alpha\text{-Cu}_{2-\delta}\text{Se}$ ($\delta = 0, 0.04, 0.2$).

Nominal	Refined	Occ.(8c)	Occ.(32f)	a (\AA)
$\text{Cu}_{1.8}\text{Se}$	$\text{Cu}_{1.72(5)}\text{Se}$	0.62(1)	0.060(4)	5.7761(1)
$\text{Cu}_{1.96}\text{Se}$	$\text{Cu}_{1.83(5)}\text{Se}$	0.58(1)	0.084(4)	5.8387(2)
Cu_2Se	$\text{Cu}_{1.84(5)}\text{Se}$	0.59(1)	0.083(4)	5.8465(3)

refinement reveals a large amount of Cu ions occupying the $8c$ sites and a small amount on the $32f$ sites. The occupancy on the $8c$ sites is anticorrelated with the total amount of the Cu content, while the occupancy on the $32f$ sites increases for the compounds with higher Cu content. Table I summarizes the structure refinement results at 430 K for $\alpha\text{-Cu}_{2-\delta}\text{Se}$. The position parameters of Cu($32f$) ions are $x = 0.331(1)$, $0.332(1)$, and $0.337(1)$ for $\text{Cu}_{1.8}\text{Se}$, $\text{Cu}_{1.96}\text{Se}$, and Cu_2Se , respectively,

in agreement with the reported results in the range of $x = 0.33 - 0.39$ ^{10,17,18,30,31}. The refined content of Cu ions as shown in Table I slightly deviates from the nominal quantity. Refinement results using the Model III are shown in Figs. 1(g)-1(i). The refinement agreement parameters are worse than those of the Model I. In addition, the refinement will result in an unreasonable thermal vibration factor $B \sim 40 \text{ \AA}^2$ for the Cu ions on the $4b$ sites. A typical value of B should be below 5 \AA^2 . The simulated NPD patterns using the Model II are very close to that of Model I. There is one additional freedom of the Cu sites for the Model II. The refinement agreement is expected to be better. However, the refinement using the Model II also yields an unreasonable $B \sim 30 \text{ \AA}^2$ for the Cu ions on the $4b$ sites. When the magnitude of B is enforced to be below 5 \AA^2 , the resultant occupancy of Cu on the $4b$ sites is in the range of $1 \sim 3\%$. Thus, our refinements reveal that the Model I agrees with the structure of the high temperature superionic α -phase $\text{Cu}_{2-\delta}\text{Se}$ the best.

We conducted QENS measurements on the same sam-

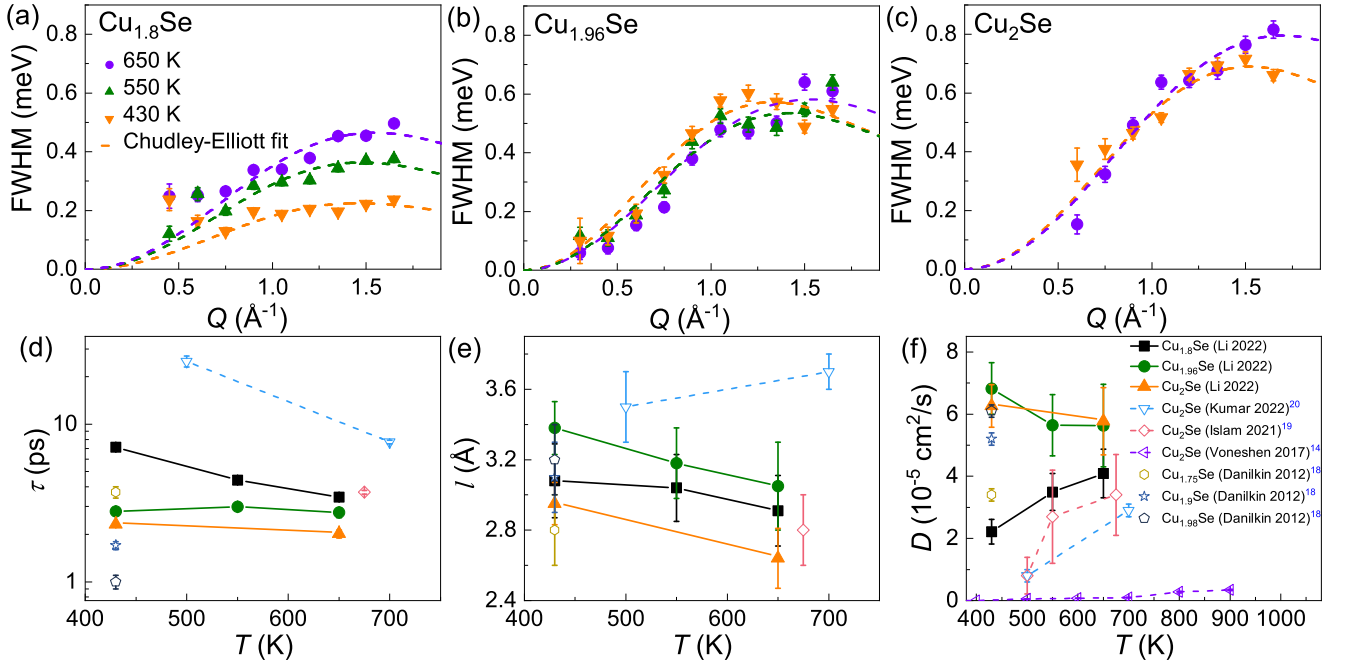


FIG. 3: Q dependence of the FWHM for (a) $\text{Cu}_{1.8}\text{Se}$, (b) $\text{Cu}_{1.96}\text{Se}$, and (c) Cu_2Se measured at 430, 550, and 650 K. The dashed lines are fittings to the C-E function. Temperature dependence of (d) the residence time τ , (e) the average jump length l , and (f) the diffusion coefficient D in $\alpha\text{-Cu}_{2-\delta}\text{Se}$. The solid symbols refer to the results of this work. Results of (Kumar 2022) are reproduced with permission from Phys. Rev. Mater. 6, 055403 (2022)²⁰. Copyright 2022 American Physical Society. Results of (Islam 2021) are reproduced with permission from Acta Mater. 215, 117026 (2021)¹⁹. Copyright 2022 Elsevier. Results of (Voneshen 2017) are reproduced with permission from Phys. Rev. Lett. 118, 145901 (2017)¹⁴. Copyright 2017 American Physical Society. Results of (Danilkin 2012) are reproduced with permission from Solid State Ionics 225, 190 (2012)¹⁸. Copyright 2012 Elsevier.

ples at 430, 550, and 650 K to investigate the diffusion behaviors microscopically. QENS experiments measure the dynamic process of individual atom such as rotation, reorientation, and diffusion in materials^{36,37}. The QENS spectra for α -phase $\text{Cu}_{2-\delta}\text{Se}$ ($\delta = 0, 0.04, 0.2$) at 430 K are shown in Fig. 2. Strong broadening QENS signals around the elastic line are observed in all compounds, where $\text{Cu}_{2-\delta}\text{Se}$ are in the superionic phase. The signals extend up to 9 meV in the energy gain side and the intense signals above $Q = 2 \text{ \AA}^{-1}$ should correspond to phonons of the samples.

The dynamic structure factor $S(Q, \omega)$ for the diffusion process has been fitted by the following formula³⁶:

$$S(Q, \omega) = [A_0(Q)\delta(\omega) + \sum_i A_i(Q)L_i(\omega)] \otimes R(Q, \omega), \quad (1)$$

where $A_0(Q)$ is the incoherent elastic structure factor, $\delta(\omega)$ is the delta function, $A_i(Q)$ is a quasi-elastic component, and $L_i(\omega)$ is a Lorentzian function. The integer i corresponds to different diffusion mode. The resolution function $R(Q, \omega)$ can be determined via the identical cuts from measurements on vanadium. The $S(Q, \omega)$ are fitted using two Lorentzian functions for all the momentum transfer Q of the QENS data as in previous reports^{19,20}. Figure 2 (d) displays a constant Q cut and the QENS peak fitting results at $Q = 1.2 \pm 0.075 \text{ \AA}^{-1}$ at 430 K

for $\text{Cu}_{1.8}\text{Se}$. The resultant two Lorentzian functions correspond to two diffusion modes with different properties. The FWHM of the narrower Lorentzian function is Q dependent and corresponds to a long-range diffusion mode. The broader Lorentzian function is independent of Q with the FWHM around $7 \pm 2 \text{ meV}$. It represents a confined mode that corresponds to short range diffusion between the nearest $8c$ and $32f$ sites of Cu ions¹⁹. Adopting one Lorentzian function and a flat background as in previous reports is also tested in our analyses^{17,18}. In this way, the FWHMs of the single Lorentzian function are similar to the narrower Lorentzian function corresponding to the long-range diffusion mode. However, the information of the confined mode is lost. The QENS spectra and analyses for the samples at 550 and 650 K are not presented in Fig. 2.

Figure 3(a) displays the FWHMs of the narrower Lorentzian function as a function of Q , yielding that the QENS peaks become broader as the temperature increases for $\text{Cu}_{1.8}\text{Se}$. Increasing of the Cu content also broadens the FWHMs as shown in Figs. 3(b) and 3(c) for $\text{Cu}_{1.96}\text{Se}$ and Cu_2Se . While the FWHMs for the two compounds with more Cu content are almost temperature independent. An isotropic C-E model is employed to analyze the diffusion process of $\alpha\text{-Cu}_{2-\delta}\text{Se}$ ²¹. In this model, isotropic long-range diffusions can be regarded as

a successive jump of mobile atoms between the adjacent crystallographic sites. The C-E model is given by

$$\text{FWHM}(Q) = \frac{2\hbar}{\tau} \left(1 - \frac{\sin(Ql)}{Ql}\right) \quad (2)$$

where l is the average jump length and τ is the residence time of an atom at each site. Accordingly, the diffusion coefficient D is expressed as $D = \frac{l^2}{2d\tau}$, where $d = 3$ is the dimensional number for the three dimensional diffusion in α -Cu_{2- δ} Se. The fits of FWHM to the C-E model are displayed in Figs. 3(a)-3(c). The resultant temperature dependence of τ , l , and D are shown in Figs. 3(d)-3(f).

The residence time τ in Fig. 3(d) is on the scale of 10^{-12} s in agreement with previous reports^{14,17-20}. As temperature increases, τ is expected to become shorter due to the thermal fluctuations as it is indeed observed in Cu_{1.8}Se. However, the τ for Cu_{1.96}Se and Cu₂Se does not change obviously in this temperature range. The temperature dependence of the residence time is related to the diffusion activation energy and may also have connections to the occupancies of the 8c and 32f sites¹⁹. As one can deduce from the residence time (~ 2 ps), the Cu diffusion process is fast and can only affect the phonon spectra below 2 meV. Thus, the phonon anharmonicity or the dynamic creation and destruction of the Frenkel defects may be responsible for the ultra-low thermal conductivity in α -Cu₂Se^{14,19}.

The average jump lengths l obtained from the fitting are in the range of 2.7 – 3.4 Å as shown in Fig. 3(e). The analysis of the diffusion paths depends on the structural model. In our NPD refinement, the Cu ions are determined to occupy the 8c and 32f sites. The nearest and next nearest distances for the 8c sites of Cu_{1.96}Se at 430 K are 2.919(1) and 4.128(1) Å, respectively. These distances are close in the compounds of α -Cu_{2- δ} Se ($\delta = 0, 0.04, 0.2$). Thus, the hopping between the adjacent 8c sites may be the main long-range diffusion mode which can be captured well by the average jump length l . Because the occupancy of the 32f site increases as the diffusion coefficient, the 32f site is likely a bypass in the long-range diffusion process^{17,18}. The confined mode can be attributed to the localized hopping between the nearest 8c and 32f sites for Cu ions. Thus, the two diffusion modes cooperate as theoretical simulations³⁸.

The diffusion coefficient reflects diffusion rate in a diffusion process. Figure 3(f) displays the diffusion coefficient D as a function of temperature. The magnitude of D on the scale of 10^{-5} cm²/s is consistent with most of the QENS results¹⁷⁻²⁰, while in contrast to that determined from the chemical measurements which are in the magnitudes of 10^{-4} or 10^{-6} cm²/s^{15,16,39}. Since the average jump length l is nearly temperature independent, the D is enhanced by thermal fluctuations as expected in Cu_{1.8}Se. For Cu_{1.96}Se and Cu₂Se, the D is larger,

which may result from the stronger correlations between Cu ions in the compounds with higher Cu content. However, the diffusion coefficients do not increase obviously for the two compounds with increasing temperature. The copper occupancy of the 32f sites increases with temperature with a simultaneous decrease in the 8c sites³¹. The effect of increasing temperature on the Cu occupancies of the two sites is similar with increasing the nominal Cu content. The enhanced Cu occupancy on the 32f sites by the nominal Cu content may suppress further improving of the Cu occupancy on the same sites by temperature in this range. We note the compositions summarized in Fig. 3(f) are nominal, which may deviate from the actual compositions. Voneshen et. al. separated the diffusion modes in a different way. The diffusion coefficient could not compare with the others directly¹⁴.

In summary, the average crystal structure and the diffusion behaviors of superionic α -Cu_{2- δ} Se ($\delta = 0, 0.04, 0.2$) have been studied by NPD and QENS. The Cu ions for α -Cu_{2- δ} Se occupy on the tetrahedral 8c and trigonal 32f sites. A long-range diffusion mode and a confined mode are extracted through the analyses of the QNES spectra. In the long-range diffusion mode, the residence time τ is on the time scale of picosecond. The jump length l can capture the main jump pathway of hopping between nearest 8c sites for the long-range diffusion. The confined mode corresponds to the localized hopping between the nearest 8c and 32f sites. The long-range diffusion coefficient is on the scale of $\sim 10^{-5}$ cm²/s and increases with elevating temperature for the compounds with a lower Cu content. The diffusion coefficient increases for the compounds with higher Cu content. However, the diffusion rates for compounds with higher Cu content are almost temperature independent, which could be attributed to the compensation of temperature and nominal Cu content on the occupancies of the 8c and 32f sites. The Cu occupancy on the 32f site has an obvious connection to the diffusion properties of the long-range mode, consistent with the 32f site as a bypass site in the long-range diffusion process. Thus, the two diffusion modes cooperate. These outcomes provide important insights for the understanding of the Cu ions diffusion in superionic α -Cu_{2- δ} Se, and shed a light on further investigation of liquid-like thermoelectric materials.

We thank ANSTO for providing access to Echidna and Pelican (Proposal ID P6942) at the Australian Center for Neutron Scattering. Work at Sun Yat-Sen University was supported by the National Natural Science Foundation of China (Grants No. 12174454, No. 11904414), the Guangdong Basic and Applied Basic Research Foundation (No. 2021B1515120015), and the National Key Research and Development Program of China (Grant No. 2019YFA0705702).

- * Electronic address: wangmeng5@mail.sysu.edu.cn
- ¹ J. He and T. M. Tritt, *Science* **357**, 1369 (2017).
 - ² A. F. Ioffe, L. S. Stil, E. K. Iordanishvili, T. S. Stavitskaya, A. Gelbtuch, and G. Vineyard, *Phys. Today* **12**, 42 (1959).
 - ³ T. M. Tritt and M. A. Subramanian, *MRS Bull.* **31**, 188 (2006).
 - ⁴ L.-D. Zhao, S.-H. Lo, Y. Zhang, H. Sun, G. Tan, C. Uher, C. Wolverton, V. P. Dravid, and M. G. Kanatzidis, *Nature* **508**, 373 (2014).
 - ⁵ K. F. Hsu, S. Loo, F. Guo, W. Chen, J. S. Dyck, C. Uher, T. Hogan, E. K. Polychroniadis, and M. G. Kanatzidis, *Science* **303**, 818 (2004).
 - ⁶ J. P. Heremans, V. Jovovic, E. S. Toberer, A. Saramat, K. Kurosaki, A. Charoenphakdee, S. Yamanaka, and G. J. Snyder, *Science* **321**, 554 (2008).
 - ⁷ G. Rogl, A. Grytsiv, P. Rogl, N. Peranio, E. Bauer, M. Zehetbauer, and O. Eibl, *Acta Mater.* **63**, 30 (2014).
 - ⁸ H. Liu, X. Shi, F. Xu, L. Zhang, W. Zhang, L. Chen, Q. Li, C. Uher, T. Day, and G. Snyder Jeffrey, *Nat. Mater.* **11**, 422 (2012).
 - ⁹ M. Li, D. L. Cortie, J. Liu, D. Yu, S. M. K. N. Islam, L. Zhao, D. R. Mitchell, R. A. Mole, M. B. Cortie, S. Dou, et al., *Nano Energy* **53**, 993 (2018).
 - ¹⁰ A. Tonejc, *J. Mater. Sci.* **15**, 3090 (1980).
 - ¹¹ M. A. Korzhuev, V. F. Bankina, B. F. Gruzinov, and G. S. Bushmarina, *Sov. Phys. Semicond.* **23**, 959 (1989).
 - ¹² S. A. Danilkin, *J. Alloys Compd.* **467**, 509 (2009).
 - ¹³ K. Zhao, P. Qiu, X. Shi, and L. Chen, *Adv. Funct. Mater.* **30**, 1903867 (2020).
 - ¹⁴ D. J. Voneshen, H. C. Walker, K. Refson, and J. P. Goff, *Phys. Rev. Lett.* **118**, 145901 (2017).
 - ¹⁵ R. Yakshibaev, V. Konev, and M. Balapanov, *Sov. Phys. Solid State* **26**, 2189 (1984).
 - ¹⁶ M. Korzhuev, *Sov. Phys. Solid State* **31**, 1666 (1989).
 - ¹⁷ S. A. Danilkin, M. Avdeev, T. Sakuma, R. Macquart, C. D. Ling, M. Rusina, and Z. Izaola, *Ionics* **17**, 75 (2011).
 - ¹⁸ S. A. Danilkin, M. Avdeev, M. Sale, and T. Sakuma, *Solid State Ionics* **225**, 190 (2012).
 - ¹⁹ S. M. K. Nazrul Islam, P. Mayank, Y. Ouyang, J. Chen, A. K. Sagotra, M. Li, M. B. Cortie, R. Mole, C. Cazorla, D. Yu, et al., *Acta Mater.* **215**, 117026 (2021).
 - ²⁰ S. Kumar, M. K. Gupta, P. Goel, R. Mittal, O. Delaire, and A. Thamizhavel, *Phys. Rev. Mater.* **6**, 055403 (2022).
 - ²¹ C. T. Chudley and R. J. Elliott, *Proc. Phys. Soc.* **77**, 353 (1961).
 - ²² H. Liu, J. Yang, X. Shi, S. A. Danilkin, D. Yu, C. Wang, W. Zhang, and L. Chen, *J. Materiomics* **2**, 187 (2016).
 - ²³ M. Avdeev and J. R. Hester, *J. Appl. Cryst.* **51**, 1597 (2018).
 - ²⁴ H. M. Rietveld, *J. Appl. Cryst.* **2**, 65 (1969).
 - ²⁵ D. Yu, R. Mole, T. Noakes, and S. Kennedy, *J. Phys. Soc. Jpn.* **82**, SA027 (2013).
 - ²⁶ D. Richard, M. Ferrand, and G. J. Kearley, *J. Neutron Res.* **4**, 33 (1996).
 - ²⁷ O. MILAT, Z. VUČIĆ, and B. RUŠČIĆ, *Solid State Ionics* **23**, 37 (1987).
 - ²⁸ S. Kashida and J. Akai, *J. Phys. C: Solid State Phys.* **21**, 5329 (1988).
 - ²⁹ N. Frangis, C. Manolik, and S. Amelinc, *Phys. Stat. Sol.* **126**, 9 (1991).
 - ³⁰ R. D. Heyding and R. M. Murray, *Can. J. Chem.* **54**, 841 (1976).
 - ³¹ A. N. Skomorokhov, D. M. Trots, M. Knapp, N. N. Bickulova, and H. Fuess, *J. Alloys Compd.* **421**, 64 (2006).
 - ³² J. B. Boyce, T. M. Hayes, and J. C. Mikkelsen, *Solid State Ionics* **5**, 497 (1981).
 - ³³ M. Oliveria, R. McMullan, and B. Wuensch, *Solid State Ionics* **28**, 1332 (1988).
 - ³⁴ K. Yamamoto and S. Kashida, *J. Solid State Chem.* **93**, 202 (1991).
 - ³⁵ K. Yamamoto and S. Kashida, *Solid State Ionics* **48**, 241 (1991).
 - ³⁶ R. Hempelmann, *Quasielastic neutron scattering and solid state diffusion* (Clarendon Press, 2000).
 - ³⁷ J. P. Embs, F. Juranyi, and R. Hempelmann, *Z. Phys. Chem.* **224**, 5 (2010).
 - ³⁸ K. Zhuo, J. Wang, J. Gao, U. Landman, and M. Y. Chou, *Phys. Rev. B* **102**, 064201 (2020).
 - ³⁹ V. Konev, V. Chebotin, and S. Fomenkov, *Inorg. Mater.* **21**, 166 (1985).